

Proton Transfer Reactions of Methylanthracene Radical Cations with Pyridine Bases under Non-Steady-State Conditions. Real Kinetic Isotope Effect Evidence for Extensive Tunneling

Yun Lu, Yixing Zhao, and Vernon D. Parker*

Contribution from the Department of Chemistry and Biochemistry, Utah State University, Logan, Utah 84322-0300

Received January 30, 2001

Abstract: The kinetics of the proton transfer reactions between the 9-methyl-10-phenylanthracene radical cation (MPA^{•+}) with 2,6-lutidine were studied in acetonitrile–Bu₄NBF₄ (0.1 M) using derivative cyclic voltammetry. Comparisons of extent of reaction–time profiles with theoretical data for both the simple single-step proton transfer and a mechanism involving the formation of a donor–acceptor complex prior to unimolecular proton transfer were made. The experimental extent of reaction–time profiles deviated significantly from those simulated for the single-step mechanism, while excellent fits of experimental to theoretical data, in the *pre-steady-state* period, for the complex mechanism were observed. In this time period, the apparent deuterium kinetic isotope effects (KIE_{app}) were observed to vary significantly with the extent of reaction as predicted by the complex mechanism. Resolution of the apparent rate constants into the microscopic rate constants for the complex mechanism resulted in a real kinetic isotope effect (KIE_{real}) equal to 82 at 291 K. Arrhenius activation parameters (252–312 K) for the reactions of MPA^{•+} with 2,6-lutidine in acetonitrile–Bu₄NBF₄ (0.1 M) revealed $E_a^D - E_a^H$ equal to 2.89 kcal/mol and A^D/A^H equal to 2.09. In this temperature range, KIE_{real} varied from 46 at the highest temperature to 134 at the lowest. The large KIE_{real}, along with the Arrhenius parameters, are indicative of extensive tunneling for the proton transfer steps.

Introduction

Proton tunneling is frequently encountered in proton transfer reactions of C–H and other acids.¹ The most usual experimental observations, interpreted as indications of the phenomenon, are deuterium kinetic isotope effects which exceed about 10 at 298 K. The Arrhenius activation parameters can provide strong supporting evidence for proton tunneling. Bell¹ provided benchmark values to distinguish between processes involving proton tunneling and those following the classical model. These are Arrhenius activation energy differences ($E_a^D - E_a^H$) that exceed 1.4 kcal/mol and ratios of the Arrhenius A factors (A^D/A^H) greater than unity. We have shown that the proton transfer reactions of some methylanthracene radical cations (ArCH₃^{•+}) with pyridine bases follow a complex mechanism involving the formation of kinetically significant intermediate complexes prior to unimolecular proton transfer.^{2,3} These reactions do not reach the steady state until late in the first half-life, which allows the kinetics of the reactions to be resolved in the pre-steady-state time period. To accomplish the later, it is necessary to carry out concurrent analysis of kinetic data for both ArCH₃^{•+} and ArCD₃^{•+}.³ We reported kinetic isotope effects for several of these reactions in dichloromethane–Bu₄NPF₆ (0.2 M) ranging from 31 to 47, providing evidence for proton tunneling.³ In this paper we present detailed studies of the kinetics of the reactions between the 9-methyl-10-phenylanthracene radical cation (MPA^{•+}) and 2,6-lutidine (2,6-LUT) at temperatures ranging from 252

to 312 K which strongly implicate extensive proton tunneling in this reaction.

More recently, we have shown that accessing the pre-steady-state to resolve the kinetics of proton transfer reactions is not restricted to electrode kinetic studies of radical cations but can also be achieved in stopped-flow kinetic studies of proton transfer reactions of 1-nitro-1-(4-nitrophenyl)ethane with hydroxide ion.⁴ The latter study resulted in the observation of real deuterium kinetic isotope effects ranging from 17 to 26 as well as Arrhenius parameters consistent with proton tunneling ($E_a^D - E_a^H = 2.8$ kcal/mol; $A^D/A^H = 4.95$).

Results

The reaction between MPA^{•+} and 2,6-LUT in acetonitrile–Bu₄NPF₆ (0.1 M) takes place at rates convenient to follow the kinetics by derivative cyclic voltammetry.⁵ A factor of importance in the study of proton transfer reactions is the position of equilibrium. We have recently pointed out that in order to avoid the complications accompanying D/H exchange, proton transfer reactions must lie far to the right.⁴ The pK_a of MPA^{•+} in acetonitrile⁶ has been estimated to be equal to 3 from the value determined in dimethyl sulfoxide⁷ while that for 2,6-LUT in acetonitrile⁸ has been reported to be 15.4. The difference in pK_a values corresponds to an equilibrium constant of about 10¹² for

(1) Bell, R. P. *The Tunnel Effect in Chemistry*; Chapman and Hall: London, 1980.

(2) Parker, V. D.; Chao, Y.-T.; Zheng, G. *J. Am. Chem. Soc.* **1997**, *119*, 11390.

(3) Parker, V. D.; Zhao, Y.; Lu, Y.; Zheng, G. *J. Am. Chem. Soc.* **1998**, *120*, 12720.

(4) Zhao, Y.; Lu, Y.; Parker, V. D. *J. Am. Chem. Soc.* **2001**, *123*, 1579.

(5) Parker, V. D. *Electroanal. Chem.* **1986**, *14*, 1.

(6) Parker, V. D.; Chao, Y.-T.; Reitstoen, B. *J. Am. Chem. Soc.* **1991**, *113*, 2336.

(7) Cheng, J.-P. Ph.D. Dissertation, Northwestern University, 1987.

(8) Billon, J. P.; Cauquis, G.; Raison, J.; Thibaud, Y. *Bull. Soc. Chim. Fr.* **1967**, 199.

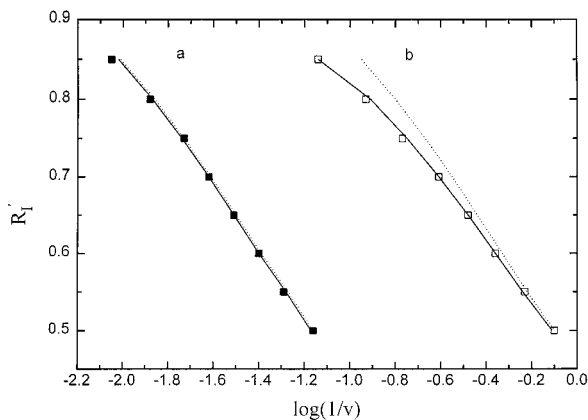
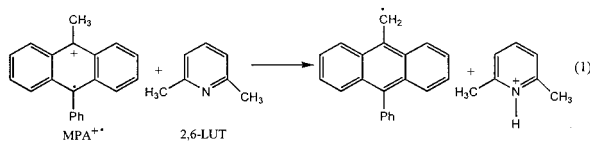
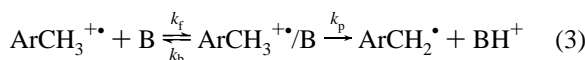


Figure 1. Theoretical DCV data at 291.5 K for the reactions of MPA⁺• (solid squares) and MPA-*d*₃⁺• (open squares) with 2,6-LUT as a function of voltage sweep rate. The dashed lines are theoretical data for the simple second-order mechanism, and the solid lines represent theoretical data for the two-step proton transfer mechanism.

reaction 1 that for all practical purposes can be assumed to be irreversible. The further product-forming reactions of the (9-phenylanthranyl)methyl radical, rapid electron transfer oxidation to the corresponding cation which reacts with 2,6-LUT to form the lutidinium ion, affect only the stoichiometry not the rate of the reaction.²



Protocol for Distinguishing between the Simple One-Step Mechanism and the Complex Mechanism for the Proton Transfer Reaction. There are distinct differences in the DCV response for the simple (eq 2) and complex (eq 3) mechanisms for proton transfer reactions. Before elaborating on these



differences, it is necessary to briefly describe how DCV is used in kinetic studies. Cyclic voltammetry, due to the difficulty of establishing a base line for the return scan, lacks the precision necessary for detailed kinetic studies. This difficulty is rectified when using the first derivative of the response and the base line for both the forward and reverse scans are close to zero.⁵ The magnitude of the derivative peaks ($R'_1 = I_b/I_f$), which provides a measure of the rate of reaction of the electrode-generated intermediate (in this case the radical cation), varies from 1.0 for no reaction to close to 0 for complete reaction during the time of the experiment. The experimental variable is v , the voltage sweep rate, which is a measure of the time window. The experimental R'_1 vs v profiles, which are equivalent to extent of reaction–time profiles and will be referred to as such in the following, may be compared to theoretical data for kinetic analysis as previously described.³

The first experimental mechanism test involves comparing the extent of reaction–time profiles for reactions of both ArCH₃⁺• and ArCD₃⁺• with the base (2,6-LUT in this work) to those expected for the simple mechanism. This comparison is shown in Figures 1a (ArCH₃⁺•) and 1b (ArCD₃⁺•). The data

reveal that the two experimental reaction–time profiles differ from those expected for the simple mechanism. The deviation from simple mechanism response is small for the reactions of ArCH₃⁺• but considerably larger for those of ArCD₃⁺•, and this gives rise to extent of reaction-dependent apparent kinetic isotope effects that are the criteria for the second experimental mechanism test.

The ratio of the times necessary to reach a given extent of reaction (t_D/t_H) provides a measure of the apparent deuterium kinetic isotope effect (KIE_{app}). For the simple proton transfer mechanism, KIE_{app} is equal to KIE_{real} , the deuterium kinetic isotope effect for the proton transfer step, which is independent of the extent of reaction. Plots of KIE_{app} vs R'_1 (extent of reaction) for the reactions of MPA⁺• with 2,6-LUT in acetonitrile–Bu₄NPF₆ at temperatures ranging from 252 to 312 K (solid squares) along with those expected for the simple mechanism (dashed lines) are shown in Figures 2a–d. The experimental points in all cases indicate significant extent of reaction dependences of KIE_{app} and deviate significantly from the lines projected for the simple mechanism.

It is apparent that the experimental data are inconsistent with the simple mechanism (1) with respect to both of the experimental criteria tested. Deviations from the simple mechanism response in both of these tests show that the kinetics of the reaction are consistent with the complex mechanism and provide a means to resolve the apparent rate constants into the microscopic rate constants. Although the failure of the experimental data to fit one or both of the experimental criteria does not rule out the complex mechanism, it is not possible to distinguish between the two mechanisms under these circumstances.

Fitting Experimental to Theoretical Kinetic Data for the Complex Proton-Transfer Mechanism. The extent of reaction–time profiles shown in Figure 1 as well as the KIE_{app} –extent of reaction data in Figure 2 can readily be fit to theoretical data for mechanism (3). The solid lines in the figures represent theoretical data for mechanism (3). The average deviation of the experimental points from the solid lines in Figure 1 are 2.1% for both ArCH₃⁺• and ArCD₃⁺• reactions with 2,6-LUT. The average deviations of experimental KIE_{app} values, which are ratios of experimental data, from the theoretical lines in Figure 2 are about 3%. Experimental KIE_{app} values are compared with theoretical data in Table 1. The deviations between experimental and theoretical values for mechanism (3) in both figures, as well as in Table 1, are within experimental error.

Once steady state is achieved for mechanism (3), the rate law is given by eq 4. The factor of 2 accounts for the

$$-d[\text{ArCH}_3^{+\bullet}]/dt = k_{\text{app}}[\text{ArCH}_3^{+\bullet}][\text{B}] [k_{\text{app}} = 2(k_f)(k_p)/(k_b + k_p)] \quad (4)$$

stoichiometry of the overall reaction that consumes two radical cations for each product molecule formed. The apparent rate constant (k_{app}) is the steady-state expression for mechanism (3).

We have pointed out that there may be a number of different combinations of rate constants (k_f , k_b , and k_p) which give acceptable fits for any one extent of reaction–time profile.^{3,4} Extensive analysis of theoretical data for the two-step mechanism has shown that unique fit of experimental to theoretical data can be achieved by concurrent fitting of data for both ArCH₃⁺• and ArCD₃⁺•.³ This involves the assumption that only the rate constants for proton and deuterium transfer steps (k_p^{H} and k_p^{D}) are affected by the isotopic change. The expressions for the steady-state rate constants can be rearranged to give eqs

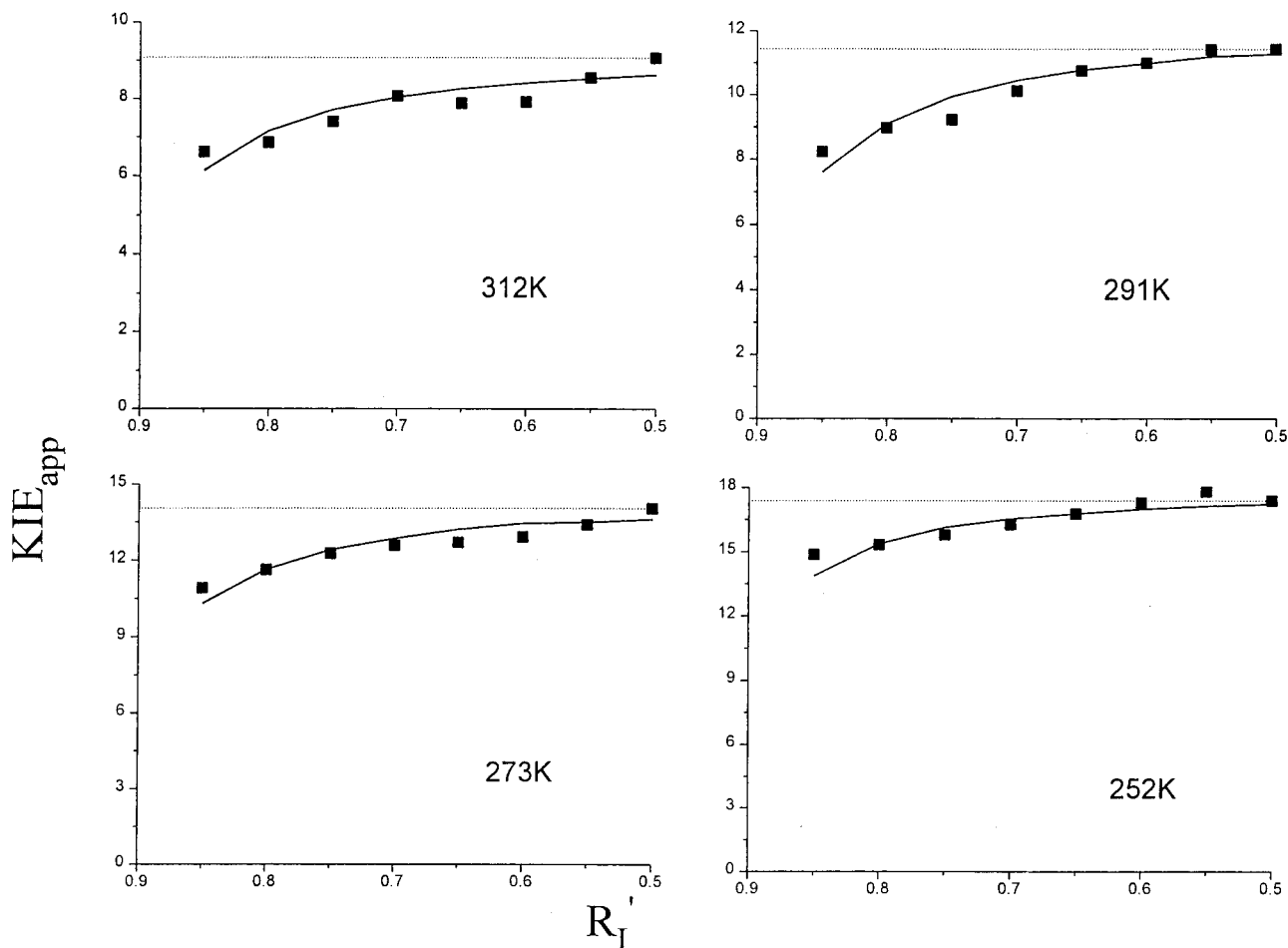


Figure 2. Apparent kinetic isotope effects as a function of extent of reaction for the reaction between MPA⁺ and 2,6-LUT at different temperatures. The solid squares represent experimental data, the dashed lines show the response expected for the simple second-order mechanism, and the solid lines are the best-fit lines for theoretical data for the two-step proton transfer mechanism.

Table 1. Dependence of Apparent Deuterium Kinetic Isotope Effects on the Temperature and the Extent of Reaction for the Reactions of MPA⁺ with 2,6-LUT in Acetonitrile–Bu₄NPF₆ (0.1 M)

R'_1	312 K		291 K		273 K		252 K	
	KIE _{app} (exp)	KIE _{app} (sim)	KIE _{app} (exp)	KIE _{app} (sim)	KIE _{app} (exp)	KIE _{app} (sim)	KIE _{app} (exp)	KIE _{app} (sim)
0.85	6.62	6.14	8.23	7.60	10.91	10.30	14.87	13.86
0.80	6.86	7.16	8.97	9.10	11.63	11.64	15.32	15.36
0.75	7.41	7.72	9.23	9.95	12.27	12.41	15.79	16.13
0.70	8.08	8.04	10.13	10.45	12.59	12.86	16.27	16.52
0.65	7.89	8.26	10.76	10.78	12.70	13.21	16.76	16.76
0.60	7.92	8.41	11.00	10.98	12.92	13.45	17.29	16.97
0.55	8.56	8.53	11.42	11.20	13.40	13.49	17.80	17.12
0.50	9.08	8.63	11.44	11.28	14.05	13.61	17.38	17.21

5 and 6 which, when combined, result in eq 7 for the real kinetic

$$(k_{\text{app}}^{\text{H}})_{\text{ss}}/2k_{\text{f}} = (k_{\text{p}}^{\text{H}}/k_{\text{b}})/(1 + k_{\text{p}}^{\text{H}}/k_{\text{b}}) = \text{CH} \quad (5)$$

$$(k_{\text{app}}^{\text{D}})_{\text{ss}}/2k_{\text{f}} = (k_{\text{p}}^{\text{D}}/k_{\text{b}})/(1 + k_{\text{p}}^{\text{D}}/k_{\text{b}}) = \text{CD} \quad (6)$$

$$\text{KIE}_{\text{real}} = [\text{CH}/(1 - \text{CH})]/[\text{CD}/(1 - \text{CD})] \quad (7)$$

isotope effect, KIE_{real}.⁹ This shows that in addition to the apparent rate constants at steady state [($k_{\text{app}}^{\text{H}}$)_{ss} and ($k_{\text{app}}^{\text{D}}$)_{ss}], it is only necessary to determine k_{f} in order to evaluate KIE_{real}.

(9) The factor of 2 in eqs 5 and 6 was omitted in ref 3. These equations, also expressed in ref 4, are correct for the stoichiometry of the nitroalkane proton transfer reactions.

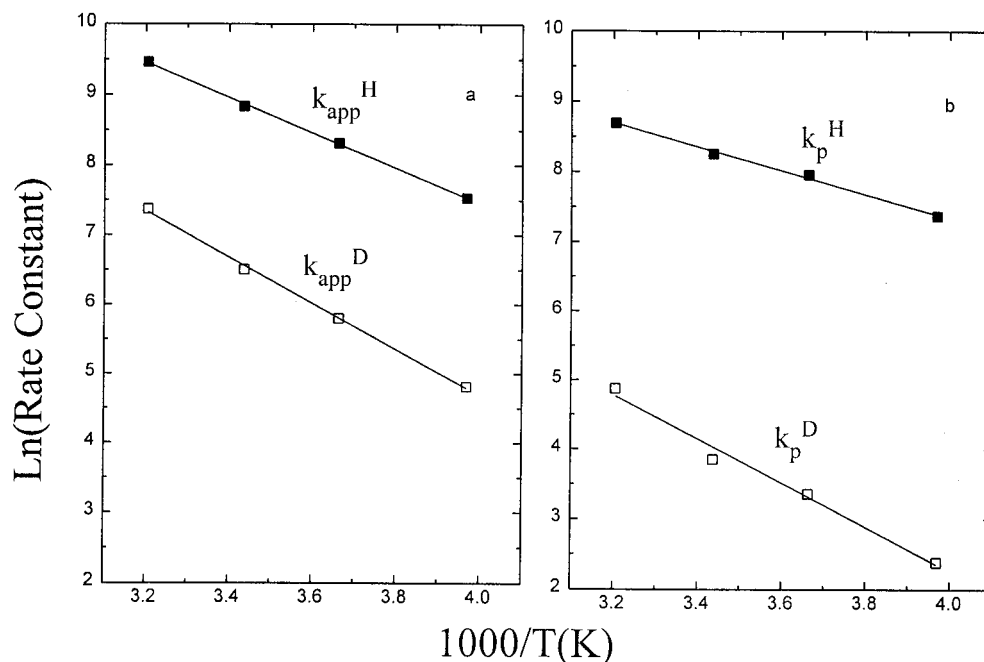
The importance of the latter will become apparent when the errors in fitting experimental to theoretical data are discussed.

Rate Constants for the Reactions of MPA Radical Cation with 2,6-Lutidine in Acetonitrile–Bu₄NPF₆ (0.1 M). The results of fitting the experimental data to theoretical data for the complex mechanism are summarized in Table 2. At each temperature, R'_1 - v data were collected with R'_1 ranging from 0.85 to 0.50. The input data for the fitting program consisted of two arrays of v values (for ArCH₃⁺ and for ArCD₃⁺), those necessary for R'_1 to equal 0.85 down to 0.50 in 0.05 intervals, along with the apparent rate constants measured at R'_1 equal to 0.50.

The identity of all of the rate constants but one is obvious from the preceding discussion. This rate constant, for reaction

Table 2. Temperature Dependence of the Complex Mechanism Rate Constants for the Reactions of MPA⁺⁺ with 2,6-LUT in Acetonitrile–Bu₄NPF₆ (0.1 M)

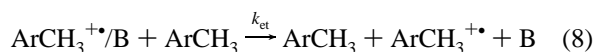
T/K	$k_{\text{app}}^{\text{H}}/\text{M}^{-1}\text{s}^{-1}$	$k_{\text{app}}^{\text{D}}/\text{M}^{-1}\text{s}^{-1}$	$k_{\text{f}}/\text{M}^{-1}\text{s}^{-1}$	$k_{\text{b}}/\text{s}^{-1}$	$k_{\text{p}}^{\text{H}}/\text{s}^{-1}$	$k_{\text{p}}^{\text{D}}/\text{s}^{-1}$	$k_{\text{et}}/\text{M}^{-1}\text{s}^{-1}$	KIE _{real}
312	12 830	1586	15 250	1126	5970	130.6	53 800	46
291	6860	665	7750	499	3850	46.9	47 600	82
273	4080	329	4570	344	2864	28.6	37 200	108
252	1865	122.6	2090	190.9	1582	10.81	32 800	134

**Figure 3.** Arrhenius plots for second-order apparent rate constants (a) and first-order rate constants (b) for the proton and deuteron transfer reactions of MPA⁺⁺ and MPA-d₃⁺⁺ with 2,6-LUT.**Table 3.** Apparent and Real Arrhenius Activation Parameters for the Reactions of MPA⁺⁺ with 2,6-LUT in Acetonitrile–Bu₄NPF₆ (0.1 M)

	apparent ^a		real ^b	
	H	D	H	D
E_a (kcal/mol)	4.99	6.62	3.40	6.29
$E_a^{\text{D}} - E_a^{\text{H}}$ (kcal/mol)	1.63		2.89	
$10^{-6}A$	39.8	64.6	1.42	2.96
$A^{\text{D}}/A^{\text{H}}$	1.62		2.09	

^a Derived from $k_{\text{app}}^{\text{H}}$ and $k_{\text{app}}^{\text{D}}$. ^b Derived from k_{p}^{H} and k_{p}^{D} .

8, is of minor importance in the overall scheme but must be



taken into account for the precise fitting of the data. The redox potential of ArCH₃⁺⁺/B is expected to be³ a few millivolts less positive than that of ArCH₃⁺⁺ so reaction 8 does account for some decomposition of the radical cation/base complex. Neglect of reaction 8 brings about only small changes in the other rate constants.

Another feature of interest in the data in Table 2 is the magnitude of KIE_{real}, which varies from 48 to 134 in the temperature range from 312 to 252 K. In this temperature range KIE_{app} varies from about 7 to 17 (Table 1).

Arrhenius Parameters for the Reaction of MPA Radical Cation with 2,6-Lutidine in Acetonitrile–Bu₄NPF₆ (0.1 M). Arrhenius plots for $k_{\text{app}}^{\text{H}}$, $k_{\text{app}}^{\text{D}}$, k_{p}^{H} , and k_{p}^{D} are illustrated in Figure 3. Apparent and real Arrhenius parameters are summarized in Table 3. The activation energy differences and $A^{\text{D}}/A^{\text{H}}$

Table 4. Effect of Fitting Errors in Rate Constants on the Quality of Experimental to Theoretical R'_1 -Sweep Rate Data Fits

rate constant	Δ_{total}	Δ_{H}	Δ_{D}	Δ_{KIE}
best fit	7.15	2.10	2.08	2.97
$(k_{\text{app}}^{\text{H}}/\text{M}^{-1}\text{s}^{-1}) + 1\%$	7.70	2.09	2.86	2.97
$(k_{\text{app}}^{\text{H}}/\text{M}^{-1}\text{s}^{-1}) - 1\%$	8.58	2.34	2.99	3.25
$(k_{\text{app}}^{\text{D}}/\text{M}^{-1}\text{s}^{-1}) + 1\%$	7.51	2.10	2.20	3.22
$(k_{\text{app}}^{\text{D}}/\text{M}^{-1}\text{s}^{-1}) - 1\%$	7.81	2.10	2.52	3.20
$(k_{\text{f}}/\text{M}^{-1}\text{s}^{-1}) + 1\%$	7.86	2.09	2.79	2.98
$(k_{\text{f}}/\text{M}^{-1}\text{s}^{-1}) - 1\%$	7.44	2.10	2.06	3.28
$(k_{\text{p}}/\text{M}^{-1}\text{s}^{-1}) + 10\%$	8.11	2.11	3.04	2.96
$k_{\text{p}}/\text{M}^{-1}\text{s}^{-1} - 10\%$	7.72	2.08	2.12	3.52
$k_{\text{et}}/(\text{M}^{-1}\text{s}^{-1}) + 10\%$	7.30	2.10	2.20	3.00
$k_{\text{et}}/(\text{M}^{-1}\text{s}^{-1}) - 10\%$	7.20	2.10	2.07	3.03

A^{H} derived from both apparent and microscopic rate constants exceed the values expected for the classical model.

Uncertainty in Rate Constants Derived from the Fitting Procedure. The average deviations of experimental points from the theoretical fitting lines, for example, those in Figure 1, are about 2% which is within the experimental error for the measurement of R'_1 . The deviations from the theoretical fitting lines for KIE_{app} (Figure 2 and Table 1), which are ratios of the H and D points from Figure 1, are slightly greater at about 3% but are also within experimental error by virtue of the data from which they are derived.

The effect of changes in rate constants on the percent deviations between experimental and theoretical data is illustrated in Table 4. The first line in Table 4 summarizes the various percent deviations, Δ_{total} , Δ_{H} , Δ_{D} , and Δ_{KIE} (eq 9), for the best fit between experimental points measured at 291 K and theoretical data for the complex mechanism. The terms on the

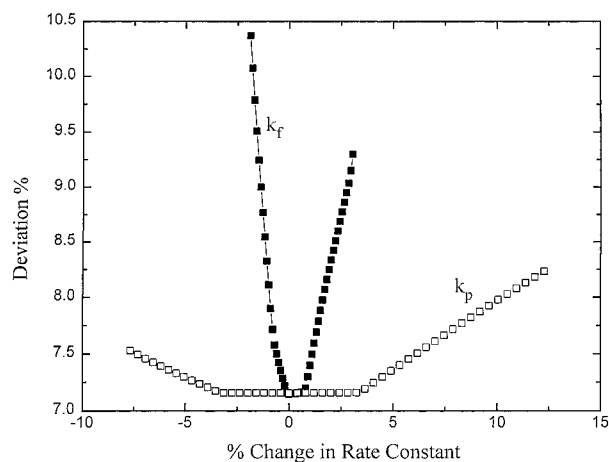


Figure 4. Plots showing percent deviation of theoretical to experimental data caused by changes in rate constants from the best-fit values: k_f (solid squares) and k_p (open squares).

right-hand side of eq 9 refer to the percent deviation between

$$\Delta_{\text{total}} = \Delta_{\text{H}} + \Delta_{\text{D}}\Delta_{\text{KIE}} \quad (9)$$

experimental and theoretical data for the extent of reaction–time profile for proton transfer (Δ_{H}), that for deuteron transfer (Δ_{D}), and that for KIE_{app} (Δ_{KIE}). The remainder of the table shows the effect of varying a single rate constant in the simulations while holding all others at the value of the best fit. Plots of any one of the percent deviations (Δ_{total} , Δ_{H} , Δ_{D} , or Δ_{KIE}) vs one of the rate constants are parabola-like with the best fit value at the minimum.³ How shallow or how steep the parabola are depend on the rate constants. From the data in Table 4 it is obvious that Δ_{total} is much more sensitive to changes in k_f , $k_{\text{app}}^{\text{H}}$, and $k_{\text{app}}^{\text{D}}$ than to changes in k_p . The sensitivity to changes in k_{et} is even lower.

The values of $k_{\text{app}}^{\text{H}}$ and $k_{\text{app}}^{\text{D}}$ obtained experimentally at $t_{1/2}$ are not the optimum values. The first step in the fitting procedure is to optimize these apparent rate constants by obtaining the best fits to the extent of reaction–time profiles. The optimized values are usually within about 2% of the experimental values. These deviations are within the normal error range for rate constant measurements by DCV.

The difference in sensitivity toward changes in k_f and k_p is further illustrated by the Δ_{total} vs rate constant profiles in Figure 4. The x -axis in Figure 4 represents the rate constants expressed as a percentage of the best fit value. At the resolution used in the graph, the lines around the minima of the two curves appear to be linear. The data in these areas of the curves actually are parabola-like and may be fit with second-order polynomial equations. When straight lines are drawn through the points of the wings of the curves in Figure 4, the two straight lines for each curve intersect at x -axis values very near zero, about 0.25% for the k_f curve and about 0.5% for the k_p curve. When the x -axis is expressed in rate constant values, this suggests that the fitting error would be 0.5% or less using this method to determine the best-fit rate constant. Obviously, an error of this magnitude for fitting experimental to theoretical data is considerably less than experimental error for the DCV measurements.

We use two different methods to locate the best fit depending upon the stage of refinement of the fit. The first method, which is used at a lower degree of fit refinement, is to select the lowest value of Δ_{total} for a series of simulations. The second, more accurate method is to treat the data as second-order polynomials

and to calculate the minima from the equations of the lines. The latter method is used in the final stages of the fitting procedure. More details of the fitting procedure may be found in ref 3.

Discussion

Methylarene radical cations hold the distinction of being among the most acidic C–H acids.^{10,11} The removal of an electron from a methylarene reduces the $\text{p}K_{\text{a}}$ of the species by as much as about 60 units and the radical cations are often superacids. The proton transfer reactions of organic radical cations have been the subject of numerous papers over the past 20 years.^{12–20} Because of the high acidity of the radical cations and the fact that the radicals resulting from proton transfer undergo rapid electron transfer oxidation, the proton transfers have most often been considered to be simple irreversible single-step processes as illustrated in eq 2. We have for several years^{2,6,12e–g} preferred a mechanism which involves the reversible formation of a radical cation/base complex followed by irreversible proton transfer as illustrated in eq 3. Until recently,³ the most compelling evidence for a complex mechanism for the proton transfer reactions of radical cations was the observation of negative apparent activation energies.^{12e,g}

(10) (a) Nicholas, A. M.; Arnold, D. R. *Can. J. Chem.* **1982**, *60*, 2165. (b) Nicholas, A. M.; Boyd, R. J.; Arnold, D. R. *Can. J. Chem.* **1982**, *60*, 3011.

(11) (a) Bordwell, F. G.; Cheng, J.-P. *J. Am. Chem. Soc.* **1989**, *111*, 1792. (b) Zhang, X.; Bordwell, F. G. *J. Org. Chem.* **1992**, *57*, 4163. (c) Zhang, X.; Bordwell, F. G.; Bares, J. E.; Cheng, J.-P.; Petrie, B. C. *J. Org. Chem.* **1993**, *58*, 3051.

(12) (a) Berek, J.; Ahlberg, E.; Parker, V. D. *Acta Chem. Scand.* **1980**, *B34*, 85. (b) R. Schmid Baumberger; Parker, V. D. *Acta Chem. Scand.* **1980**, *B34*, 537. (c) Parker, V. D. *Acta Chem. Scand.* **1985**, *B39*, 227. (d) Parker, V. D.; Tilset, M. *J. Am. Chem. Soc.* **1986**, *108*, 6371. (e) Reitstoen, B.; Parker, V. D. *J. Am. Chem. Soc.* **1990**, *112*, 4968. (f) Parker, V. D.; Tilset, M. *J. Am. Chem. Soc.* **1991**, *113*, 8778. (g) Xue, J.-Y.; Parker, V. D. *J. Org. Chem.* **1994**, *59*, 6564. (h) Parker, V. D.; Chao, Y.-T.; Zheng, G. *J. Am. Chem. Soc.* **1997**, *119*, 11390.

(13) (a) Schlesener, C. J.; Amatore, C.; Kochi, J. K. *J. Am. Chem. Soc.* **1984**, *106*, 3567. (b) Schlesener, C. J.; Amatore, C.; Kochi, J. K. *J. Am. Chem. Soc.* **1984**, *106*, 7472. (c) Schlesener, C. J.; Amatore, C.; Kochi, J. K. *J. Phys. Chem.* **1986**, *90*, 3747. (d) Sankararaman, S.; Perrier, S.; Kochi, J. K. *J. Am. Chem. Soc.* **1989**, *111*, 6448. (e) Masnovi, J. M.; Sankararaman, S.; Kochi, J. K. *J. Am. Chem. Soc.* **1989**, *111*, 2263. (f) Bockman, T. M.; Karpinski, Z. J.; Sankararaman, S.; Kochi, J. K. *J. Am. Chem. Soc.* **1992**, *114*, 1970. (g) Bockman, T. M.; Hubig, S. M.; Kochi, J. K. *J. Am. Chem. Soc.* **1998**, *120*, 2826.

(14) (a) Fukuzumi, S.; Kondo, Y.; Tanaka, T. *J. Chem. Soc., Perkin Trans. 2* **1984**, 673. (b) Fukuzumi, S.; Tokuda, Y.; Kitano, T.; Okamoto, T.; Otera, J. *J. Am. Chem. Soc.* **1993**, *115*, 8960.

(15) (a) Tolbert, L. M.; Khanna, R. K. *J. Am. Chem. Soc.* **1987**, *109*, 3477. (b) Tolbert, L. M.; Khanna, R. K.; Popp, A. E.; Gelbaum, L.; Bottomley, L. A. *J. Am. Chem. Soc.* **1990**, *112*, 2373. (c) Tolbert, L. M.; Khanna, R. K.; Popp, A. E.; Gelbaum, L.; Bottomley, L. A. *J. Am. Chem. Soc.* **1990**, *112*, 2373.

(16) (a) Dinnocenzo, J. P.; Banach, T. E. *J. Am. Chem. Soc.* **1989**, *111*, 8646. **1989**, *111*, 2263. (b) Dinnocenzo, J. P.; Karki, S. B.; Jones, J. P. *J. Am. Chem. Soc.* **1993**, *115*, 7111.

(17) (a) Baciocchi, E.; Mattioli, M.; Romano, R.; Ruzziconi, R. *J. Org. Chem.* **1991**, *56*, 7154. (b) Baciocchi, E.; Giacco, T. D.; Elisei, F. *J. Am. Chem. Soc.* **1993**, *115*, 12290. (c) Baciocchi, E.; Bietti, M.; Putignani, L.; Steenken, S. *J. Am. Chem. Soc.* **1996**, *118*, 5952. (d) Baciocchi, E.; Bietti, M.; Steenken, S. *J. Am. Chem. Soc.* **1997**, *119*, 4078. (e) Bietti, M.; Baciocchi, E.; Steenken, S. *J. Am. Chem. Soc.* **1998**, *120*, 7337. (f) Baciocchi, E.; Del Giacco, T.; Elisei, F.; Lanzalunga, O. *J. Am. Chem. Soc.* **1998**, *120*, 11800.

(18) (a) Xu, W.; Mariano, P. S. *J. Am. Chem. Soc.* **1991**, *113*, 1431. (b) Xu, W.; Zhang, X.-M.; Mariano, P. S. *J. Am. Chem. Soc.* **1991**, *113*, 8863.

(19) Steadman, J.; Syage, J. A. *J. Am. Chem. Soc.* **1991**, *113*, 6786.

(20) (a) Hapiot, P.; Moiroux, J.; Saveant, J.-M. *J. Am. Chem. Soc.* **1990**, *112*, 1337. (b) Anne, A.; Hapiot, P.; Moiroux, J.; Neta, P.; Saveant, J.-M. *J. Phys. Chem.* **1991**, *95*, 2370. (c) Anne, A.; Hapiot, P.; Moiroux, J.; Neta, P.; Saveant, J.-M. *J. Am. Chem. Soc.* **1992**, *114*, 4694. (d) Anne, A.; Fraoua, S.; Hapiot, P.; Moiroux, J.; Saveant, J.-M. *J. Am. Chem. Soc.* **1995**, *117*, 7412. (e) Anne, A.; Fraoua, S.; Grass, V.; Mouroux, J.; Saveant, J.-M. *J. Am. Chem. Soc.* **1998**, *120*, 2951.

One of the most important consequences of our findings that the kinetics of proton transfer reactions can be resolved into the rate constants for the complex mechanism, those for methylantracene radical cations³ and those for neutral nitroalkanes,⁴ is that the apparent kinetic isotope effects are not a measure of the real kinetic isotope effects for the proton transfer steps. Since kinetic isotope effects are primary tools for the investigation of reaction mechanisms and transition states, it is imperative that real kinetic isotope effects be available for analysis.

Many of the studies of proton tunneling²¹ in organic reactions have been concerned with proton transfer reactions of nitroalkanes,^{23–44} and these reactions have been treated as simple reversible second-order reactions. Since we have shown⁴ that the proton transfer reactions of a representative substrate in this series, 1-nitro-1-(4-nitrophenyl)ethane, with hydroxide take place by the complex mechanism some doubt arises as to whether the previous proton tunneling discussions have dealt with KIE_{real} or with KIE_{app} which cannot be equated to the latter for the proton transfer steps. It would appear to be of importance to study the temperature effects on resolved rate constants whenever possible to provide data for proton tunneling.

The proton transfer reactions between $\text{ArCH}_3^{+\bullet}$ and pyridine bases in dichloromethane— Bu_4NPF_6 (0.2 M), by virtue of the magnitudes of KIE_{real} , involve significant proton tunneling.³ We have chosen the reactions of $\text{MPA}^{+\bullet}$ with 2,6-LUT in acetonitrile— Bu_4NPF_6 (0.1 M) for more detailed studies of the temperature effects on the rate constants and KIE_{real} . It was mentioned earlier that the equilibrium constant for this reaction is of the order of 10^{12} , a fact that eliminates any possible complications arising from the reverse reaction. The extent of reaction—time profiles for this reaction (Figure 1) as well as the extent of reaction dependent KIE_{app} (Figure 2 and Table 1) provide convincing evidence that the reaction does not follow

(21) The introductory²² and subsequent papers in an issue of the *Ber. Bunsen-Ges. Phys. Chem.* devoted to Hydrogen Transfer: Theory and Experiment provide ready access to the more recent advances in the dynamics of proton transfer and proton tunneling.

(22) Limbach, H.-H.; Manz, J. *Ber. Bunsen-Ges. Phys. Chem.* **1998**, *102*, 289.

(23) Lewis, E. S.; Funderburk, L. H. *J. Am. Chem. Soc.* **1967**, *89*, 2322.

(24) Caldin, E. F.; Jarczewski, A.; Leffek, K. T. *Trans. Faraday Soc.* **1971**, *67*, 110.

(25) Jarczewski, A.; Leffek, K. T. *Can. J. Chem.* **1972**, *50*, 24.

(26) Kim, J.-H.; Leffek, K. T. *Can. J. Chem.* **1974**, *52*, 592.

(27) Caldin, E. F.; Mateo, S. *Chem. Commun.* **1973**, 854.

(28) Caldin, E. F.; Mateo, S. *J. Chem. Soc., Faraday Trans. 1* **1975**, *71*, 1876.

(29) Jarczewski, A.; Pruszyński, P. *Can. J. Chem.* **1975**, *53*, 1176.

(30) Caldin, E. F.; Dawson, E.; Hyde, R. M. *J. Chem. Soc., Faraday Trans. 1* **1975**, *71*, 528.

(31) Rogne, O. *Acta Chem. Scand.* **1978**, 559.

(32) Jarczewski, A.; Pruszyński, P.; Leffek, K. T. *Can. J. Chem.* **1979**, *57*, 669.

(33) Kresge, A. J.; Powell, M. F. *J. Am. Chem. Soc.* **1981**, *103*, 201.

(34) Caldin, E. F.; Mateo, S.; Warrick, P. *J. Am. Chem. Soc.* **1981**, *103*, 202.

(35) Sugimoto, N.; Sasaki, M.; Osugi, J. *J. Phys. Chem.* **1982**, *86*, 3418.

(36) Jarczewski, A.; Pruszyński, P.; Leffek, K. T. *Can. J. Chem.* **1983**, *61*, 2029.

(37) Sugimoto, N.; Sasaki, M.; Osugi, J. *Bull. Chem. Soc. Jpn.* **1984**, *57*, 366.

(38) Pruszyński, P.; Jarczewski, A. *J. Chem. Soc., Perkin Trans. 2* **1986**, 1117.

(39) Leffek, K. T.; Pruszyński, P. *Can. J. Chem.* **1988**, *66*, 1454.

(40) Galezowski, W.; Jarczewski, A. *J. Chem. Soc. Perkin Trans. 2* **1989**, 1647.

(41) Leffek, K. T.; Pruszyński, P.; Thanapaalasingham, K. *Can. J. Chem.* **1989**, *67*, 590.

(42) Kresge, A. J.; Powell, M. F. *J. Phys. Org. Chem.* **1990**, *3*, 55.

(43) Galezowski, W.; Jarczewski, A. *Can. J. Chem.* **1990**, *68*, 2242.

(44) Jarczewski, A.; Schroeder, G.; Leffek, K. T. *Can. J. Chem.* **1991**, *69*, 468.

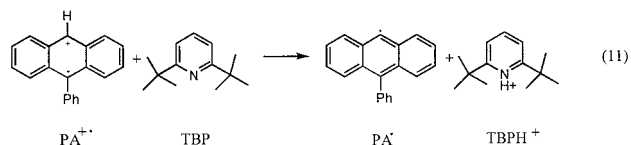
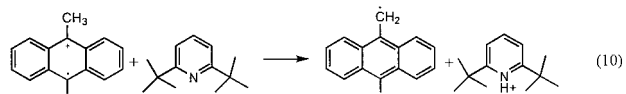
the simple reaction mechanism (2). The fact that the experimental extent of reaction—time profiles are readily fit to theoretical data generated by digital simulation for the complex mechanism (3) shows that the data are consistent with that mechanism.

The values of KIE_{real} for the reactions of $\text{MPA}^{+\bullet}$ with 2,6-LUT range from 46 (312 K) to 134 (252 K) which strongly suggest extensive proton tunneling. The Arrhenius activation parameters measured in the range from 252 to 312 K, $E^{\text{D}} - E^{\text{H}}$ equal to 2.89 and $A^{\text{D}}/A^{\text{H}}$ equal to 2.09, confirm this expectation.¹ There appears to be little doubt that the reactions follow the complex mechanism and the proton transfer is accompanied by extensive proton tunneling.

It is of interest to note that the magnitudes of KIE_{real} observed in this study as well as those previously reported³ for radical cations exceed the real kinetic isotope effects recently reported for the neutral nitroalkane carbon acids.⁴ Many of the very large kinetic isotope effects which have been reported involve unimolecular reactions of free radicals.^{45,46} As pointed out earlier,³ the reason for this may be that KIE_{app} observed for unimolecular reactions are likely to be KIE_{real} . Thus, the very large $k_{\text{H}}/k_{\text{D}}$ observed for these reactions may not be connected with the fact that the reactants are free radicals. On the other hand, it is possible that free radicals and radical cations are more prone to undergo hydrogen atom or proton transfer reactions with very large $k_{\text{H}}/k_{\text{D}}$. It would be premature to suggest the latter on the basis of the very limited KIE_{real} data available, especially for the reactions of neutral C—H proton donors.

We have previously pointed out³ that $k_{\text{H}}/k_{\text{D}}$ for proton transfer reactions of $\text{ArCH}_3^{+\bullet}$ are a combination of primary and α -secondary KIE. The latter are typically on the order of 1.15 per deuterium atom.^{47,48} This suggests that the primary KIE for the proton transfer reactions are of the order of 0.76 times (1/1.32) the total KIE_{real} .

The structure of the $\text{MPA}^{+\bullet}/2,6\text{-LUT}$ complex remains a matter of speculation. We have for some time believed that these and similar intermediates are π -complexes between the electron-deficient radical cation π -systems and the unshared electron pairs on the nitrogen-centered bases. Some support for this suggestion can be garnered from a comparison of the rate constants for the two proton transfer reactions shown below. The apparent



rate constant for reaction 10 between $\text{MPA}^{+\bullet}$ and 2,6-di-*tert*-butylpyridine (TBP) in acetonitrile— Bu_4NPF_6 (0.1 M) was observed to be equal to only $17 \text{ M}^{-1} \text{ s}^{-1}$ while that for reaction 11 between 9-phenylanthracene radical cation ($\text{PA}^{+\bullet}$) with TBP under the same conditions was reported to be equal to 130 M^{-1}

(45) Siebrand, W.; Wildman, T. A.; Zgierski, M. Z. *J. Am. Chem. Soc.* **1984**, *106*, 4089.

(46) Brunton, G.; Gray, J. A.; Griller, D.; Barclay, L. R. C.; Ingold, K. U. *J. Am. Chem. Soc.* **1978**, *100*, 4197.

(47) Streitwieser, A.; Jagow, R. H.; Fahey, R. C.; Susuki, S. *J. Am. Chem. Soc.* **1958**, *80*, 2326.

(48) Carrol, F. A. *Perspectives on Structure and Mechanism in Organic Chemistry*; Brooks/Cole: Pacific Grove, CA, 1998.

s^{-1} . The latter is highly unusual since $MPA^{+\bullet}$ is a 14 pK_a unit stronger proton donor⁶ than $PA^{+\bullet}$. The relative kinetic acidities of the two radical cations was attributed to the charge distribution in the radical cations. The aryl proton of $PA^{+\bullet}$ is directly attached to a C atom in the π -system while the arylmethyl protons in $MPA^{+\bullet}$ are remote to the latter. These observations suggest that the attraction of the unshared electron pair on nitrogen of TBP is the driving force for the formation of the radical cation–base complex. The proximity of the aryl proton of $PA^{+\bullet}$ to the nitrogen center of the base in the complex, relative to the more distant arylmethyl protons in the $MPA^{+\bullet}$ /base complex, could account for the unexpected relative proton transfer rate constants.

We have previously observed^{12h} that 9-methylanthracene radical cation, in which the 10-position is unsubstituted, undergoes nucleophilic attack at the 10-position by pyridine bases and an addition/elimination mechanism accounts for the overall proton transfer reaction. There is no evidence for this pathway in any cases where the 10-position has a substituent other than hydrogen. When the radical cation is $MPA^{+\bullet}$, the 10-position is highly hindered which precludes nucleophilic attack by 2,6-LUT.

Our conclusions, based on the resolution of the complex kinetics, on the mechanism of radical cation/base reactions are presently limited to the reactions of methylanthracene radical cations with pyridine bases. Less direct evidence is also available for a similar complex mechanism for the reactions of 9-aryl-anthracene radical cations with 2,6-di-*tert*-butylpyridine (reaction 11).^{12e,g} Arrhenius activation energies for this series of reactions^{12g} were observed to range from -2 to -11 kcal/mol. The negative E_a were interpreted to indicate the initial reversible formation of a reactant complex (negative ΔH°) followed by the product-forming reaction. Further work is necessary on this reaction to attempt to resolve the kinetics.

Conclusions

The reaction between $MPA^{+\bullet}$ and 2,6-LUT takes place by a two-step mechanism that involves the intermediate formation of a radical cation/base complex prior to unimolecular proton transfer and separation of products. Extent of reaction dependent KIE_{app} were observed at temperatures ranging from 252 to 312 K. Resolution of the kinetics of the reactions into the microscopic rate constants allowed KIE_{real} ranging from 46 to 134 to be evaluated. Arrhenius parameters for the proton and deuteron transfer steps resulted in $E_a^D - E_a^H$ equal to 2.89 kcal/mol and A^D/A^H equal 2.09. It was concluded that extensive proton tunneling is involved in the proton transfer reactions. It is proposed that the structure of the intermediate complex involves π -bonding between the unshared electron pair on nitrogen of the base with the electron-deficient π -system of the radical cation.

Experimental Part

Materials. Acetonitrile was allowed to reflux for several hours over P_2O_5 before distillation in which the middle fraction was collected. After passing through active neutral alumina, the solvent was used without further purification. Tetrabutylammonium hexafluorophosphate (Aldrich) was recrystallized from dichloromethane–ether before use. 9-Methyl-10-phenylanthracene was obtained from bromination of 9-phenylanthracene (Aldrich) in CCl_4 followed by halogen–lithium exchange using *tert*-butyllithium under an argon atmosphere and reaction with methyl iodide in THF at -78 °C. 9-Methyl-*d*₃-10-phenylanthracene was prepared in the same way using methyl-*d*₃ iodide (99.5+%) as alkylating agent. 2,6-Dimethylpyridine (99.5+% from Aldrich) was distilled under reduced pressure before use.

Instrumentation and Data Handling Procedures. Cyclic voltammetry was performed using a Princeton Applied Research (Princeton, NJ) Model 373 Potentiostat/Galvanostat driven by a Hewlett-Packard 3314A function generator. After passing through a Stanford Research Systems, Inc. Model SR640 dual channel low pass filter, the data were recorded on a Nicolet Model 310 digital oscilloscope with 12-bit resolution. The oscilloscope and function generator were controlled by a personal computer via an IEEE interface.

The current–potential curves were collected at selected trigger intervals to reduce periodic noise,⁴⁹ and 10 or more curves were averaged before treating with a frequency domain low pass digital filter and numerical differentiation. The standard deviation in R'_1 obtained in this way was observed to equal ± 0.004 .

Cyclic Voltammetry Measurements. A standard three-electrode one-compartment cell was used for all kinetic measurements. Positive feedback IR compensation was used to minimize the effects of uncompensated solution resistance. Reference electrodes were Ag/AgNO₃ (0.01 M) in acetonitrile constructed in the manner described by Moe.⁵⁰ The working electrodes, 0.2–0.8 mm Pt, were prepared by sealing wire in glass and polishing to a planar surface as described previously.⁵¹ The working electrodes were cleaned before each series of measurements with a fine polishing powder (Struers, OP-Alumina Suspension) and wiped with a soft cloth. The cell was immersed in a water bath controlled to ± 0.2 °C.

Kinetic Measurements. Rate constants were obtained by comparing derivative cyclic voltammetry⁵ data to theoretical data obtained by digital simulation. The reactions were studied using solutions ($CH_3CN/0.1$ M Bu₄NPF₆) containing substrate (1.0 mM) and base (10 mM) at temperatures ranging from 252 to 312 K. The experimental R'_1/v data were adjusted to 0.05 R'_1 intervals in the range 0.85 to 0.50 by linear log–log interpolation. We have previously observed that $\log R'_1/\log v^{-1}$ curves are nearly linear in that interval.⁵² To avoid interpolation error, several R'_1 values are recorded very close to either side of the desired value and averaged before interpolation. For example, to determine $v_{0.5}$, the voltage sweep rate where R'_1 is equal to 0.50, v values are selected to give R'_1 equal to about 0.51–0.52 and about 0.48–0.49. Ten or more determinations are made in these ranges, and the average values are then used in the interpolation. The minimum number of experimental cyclic voltammograms processed to give a single R'_1 value is 20, and most R'_1 values are derived from more than 50 experimental voltammograms. The resulting v values, for example $v_{0.85}$ or $v_{0.5}$, are directly proportional to apparent rate constants at extent of reaction corresponding to R'_1 , i.e. R'_1 equal to 0.85 or 0.50 in the examples given.⁵³

Digital Simulation. Although Digisim 2.1 (BioAnalytical Systems Inc., 2701 Kent Ave., W. Lafayette, IN 47906)⁵⁴ is the state-of-the-art software for carrying out simulation of cyclic voltammetry, we found that it is prohibitively time-consuming to carry out the massive number of simulations necessary to find the optimum fit between experimental and theoretical DCV data. Our simulation program was developed³ in order to automate theoretical data collection. The simulation program is based on Feldberg's explicit finite difference method.⁵⁵ The input for the program includes experimental values of k_{app}^H , k_{app}^D , initial experimental voltage sweep rates, any number of k_f (typically 10), and any number of k_p^H (typically 25) at each k_f . Changes in simulation k_p^H were accompanied by changes in k_b and k_p^D , maintaining consistency with eqs 5–7. The program simulates cyclic voltammograms for the reactions of both HA and DA, differentiates the resulting current–potential curves and assigns sweep rates necessary for each R'_1 beginning at 0.85 and ending at 0.50, stores these data in files for reactions of both HA and DA, and calculates and stores KIE_{app} at each R'_1 . The differentiation of the current–potential curves was accomplished using the least squares procedure of Savitzky and Golay.⁵⁶

(49) Lasson, E.; Parker, V. D. *Anal. Chem.* **1990**, *62*, 412.

(50) Moe, N. S. *Anal. Chem.* **1974**, *46*, 968.

(51) Lines, R.; Parker, V. D. *Acta Chem. Scand.* **1977**, *B31*, 369.

(52) Ahlberg, E.; Parker, V. D. *J. Electroanal. Chem.* **1981**, *121*, 73.

(53) Parker, V. D. *Acta Chem. Scand.* **1981**, *B35*, 233.

(54) Rudolph, M.; Reddy, D. P.; Feldberg, S. W. *Anal. Chem.* **1994**, *66*, 589A and references therein.

(55) Feldberg, S. W. *Electroanal. Chem.* **1969**, *3*, 199.

Each R'_1/v response curve requires about 12 simulations. When the initial iteration consists of 10 k_f , with 25 k_p at each k_f , the total number of simulations for that iteration is 6000 ($10 \times 25 \times 12 \times 2$). All of the theoretical data for the first iteration of the data fitting procedure can be obtained from a single input session. Each simulation requires about 0.1 to 5 s, depending on the simulation potential step width, on a 850 MHz personal computer.

Digisim 2.1 (DIGI) was previously used³ to test the reliability of the finite difference (FD) simulations. A comparison of the FD and DIGI simulations in the voltage sweep rate ranges where the experi-

mental data were obtained was made for several radical cation proton transfer reactions. Each pair of simulations gave R'_1 within 0.001 of each other (the experimental error in R'_1 is of the order of ± 0.004). The comparisons are summarized in Table S1 in the Supporting Information in ref 3.

Acknowledgment is made to the donors of the Petroleum Research Fund, administered by the American Chemical Society, as well as to the National Science Foundation (CHE-970835 and CHE-0074405) for support of this research.

JA010271P

(56) Savitzky, A.; Golay, M. *Anal. Chem.* **1964**, *36*, 1627.